

MICROCOPY RESOLUTION TEST CHART
NATIONAL BUREAU OF STANDARDS-1963-A

2



RESEARCH AND DEVELOPMENT TECHNICAL REPORT

CECOM-82-J071-3

**MULTIWAVELENGTH BIDIRECTIONAL
COUPLER-DECOUPLERS**

JON MYER and H.W. YEN

Hughes Research Laboratories
3011 Malibu Canyon Road
Malibu, CA 90265

March 1984

Interim Report No. 3 for Period
1 MAY 1983 - 29 FEBRUARY 1984

DISTRIBUTION STATEMENT

Approved for public release; distribution unlimited.

Prepared for
COMMUNICATIONS SYSTEMS CENTER

CECOM

**U S ARMY COMMUNICATIONS-ELECTRONICS COMMAND
FORT MONMOUTH, NEW JERSEY 07703**

AD-A147 009

DTIC FILE COPY

DTIC
ELECTE
NOV 1 1984
B

64 10 24 003

NOTICES

Disclaimers

The citation of trade names and names of manufacturers in this report is not to be construed as official Government indorsement or approval of commercial products or services referenced herein.

Disposition

Destroy this report when it is no longer needed. Do not return it to the originator.

UNCLASSIFIED

SECURITY CLASSIFICATION OF THIS PAGE (When Data Entered)

REPORT DOCUMENTATION PAGE		READ INSTRUCTIONS BEFORE COMPLETING FORM
1. REPORT NUMBER CECOM-82-J071-3	2. GOVT ACCESSION NO.	3. RECIPIENT'S CATALOG NUMBER
4. TITLE (and Subtitle) MULTIWAVELENGTH BIDIRECTIONAL COUPLER-DECOUPLERS		5. TYPE OF REPORT & PERIOD COVERED Interim Report No. 3 1 May 83 - 29 Feb 84
		6. PERFORMING ORG. REPORT NUMBER
7. AUTHOR(s) Jon Myer and H.W. Yen		8. CONTRACT OR GRANT NUMBER(s) DAAB07-82-C-J071
9. PERFORMING ORGANIZATION NAME AND ADDRESS Hughes Research Laboratories 3011 Malibu Canyon Road Malibu, CA 90265		10. PROGRAM ELEMENT, PROJECT, TASK AREA & WORK UNIT NUMBERS 1L1 62701 AH 92
11. CONTROLLING OFFICE NAME AND ADDRESS US Army Communications-Electronics Command (CECOM) Communications Systems Center (CENCOMS) ATTN: DRSEL-COM-RM-1, Fort Monmouth, NJ 07703-5202		12. REPORT DATE March 1984
		13. NUMBER OF PAGES 36
14. MONITORING AGENCY NAME & ADDRESS (if different from Controlling Office) US Army Communications-Electronic Command (CECOM) Communications Systems Center (CENCOMS) ATTN: DRSEL-COM-RM-1, Fort Monmouth, NJ 07703-5202		15. SECURITY CL. ASS. (of this report) Unclassified
		15a. DECLASSIFICATION/DOWNGRADING SCHEDULE
16. DISTRIBUTION STATEMENT (of this Report) Approved for public release; distribution unlimited.		
17. DISTRIBUTION STATEMENT (of the abstract entered in Block 20, if different from Report)		
18. SUPPLEMENTARY NOTES N/A		
19. KEY WORDS (Continue on reverse side if necessary and identify by block number) Multiwavelength Coupler-Decoupler Wavelength Division Multiplexer Fiber Optic Coupler		
20. ABSTRACT (Continue on reverse side if necessary and identify by block number) This is an exploratory program to develop, fabricate and test a family of active and passive, single and two-fiber, fiber optic multiwavelength, bidirectional, coupler-decoupler modules. The goal of the contract is to have each member of the coupler-decoupler (multiplexer-demultiplexer) family be capable of coupling energy into, and decoupling energy out of, a single optical transmission line using a minimum of four wavelengths (contd)		

DD FORM 1 JAN 73 1473

EDITION OF 1 NOV 65 IS OBSOLETE

UNCLASSIFIED

SECURITY CLASSIFICATION OF THIS PAGE (When Data Entered)

UNCLASSIFIED

SECURITY CLASSIFICATION OF THIS PAGE(When Data Entered)

for the simultaneous full duplex transmission of a minimum of four optical channels. The coupler-decoupler will be designed for low throughput loss (<5 dB per channel, per single pass) and minimum crosstalk (no more than -35 dB of the received optical signal). The modules fabricated during the program will be evaluated for their ability to meet military environmental requirements, particularly with respect to temperature. The approach uses the miniature planar Rowland spectrometer configuration recently developed at Hughes Research Laboratories (HRL) for NASA as the basic building block for constructing the coupler-decoupler required for this program, eliminating the need for collimating optics, prisms, or thin-film filters.

UNCLASSIFIED

SECURITY CLASSIFICATION OF THIS PAGE(When Data Entered)

TABLE OF CONTENTS

SECTION		PAGE
1	INTRODUCTION AND SUMMARY.....	1
2	EVALUATION OF REPLICA GRATINGS.....	7
3	PLANAR WAVEGUIDE FABRICATION.....	11
	A. Waveguide Lamination.....	11
	B. Cylindrical Rowland Surface Formation.....	12
4	INTERNAL OPTICS OF MULTIPLEXER BODY.....	15
5	THE ROWLAND CIRCLE GEOMETRY.....	18
6	COUPLER-DECOUPLER ASSEMBLY DESIGN.....	22
7	FUTURE PLANS.....	28



Accession For	
NTSC GSA&I	<input checked="" type="checkbox"/>
DFIC IAB	<input type="checkbox"/>
Unannounced	<input type="checkbox"/>
Justification	
By	
Distribution/	
Availability Codes	
Acct. no./or	
Dist.	Special
A-1	

LIST OF ILLUSTRATIONS

FIGURE		PAGE
1	Planar waveguide Rowland coupler-decoupler.....	3
2	Experimental arrangement for grating attachment evaluation.....	9
3	Output traces of a grating demultiplexer.....	10
4	Dimensions of the Rowland planar waveguide under fabrication.....	13
5	The light cone in the planar waveguide at 632.8 nm wavelength.....	16
6	The light cone in the planar waveguide at 825.5 nm wavelength.....	17
7	The Rowland Circle.....	19
8	The present Rowland multiplexer geometry.....	21
9	Typical demultiplexer assembly.....	23
10	Collected optical power from the output fiber as a function of fiber position.....	25
11	Polished end of a fiber array.....	26
12	Multiplexer network.....	29

SECTION 1

INTRODUCTION AND SUMMARY

Recent progress in the manufacture of optical fibers with a wide low-loss spectral window of 0.8 to 1.6 μm and of low-threshold, long-life semiconductor light sources covering the corresponding wavelength region has made wavelength division multiplexing (WDM) possible. The WDM technique effectively provides multiple transmission channels using a single optical fiber and enables the optical fiber to be used more efficiently. As a result, this technique is expected to increase the information capacity of a single optical fiber by realizing full duplex transmission of various types of digital and analog modulated signals.

For a WDM system, a coupler (multiplexer) and a decoupler (demultiplexer) are necessary for the transmitter and the receiver, respectively. A multiplexer consists of input fibers (each coupled to a source of a specific wavelength), a multiplexing circuit, and a transmission fiber. A demultiplexer consists of a transmission fiber, a demultiplexing circuit, and output fibers. A multiplexing circuit couples optical signals of different wavelengths to a single transmission fiber, and a demultiplexer circuit separates these optical multiple signals.

The present contract is an exploratory development program to develop, fabricate, and test a family of fiber optic, multiwavelength, bidirectional coupler-decoupler modules that can provide simultaneous full duplex transmission of a minimum of four channels over either a two-fiber or a single-fiber line. The coupler-decouplers should have low throughput loss (< 5 dB per channel, per single pass) and minimum crosstalk (< -35 dB of the received optical signal).

Our approach to the coupler-decoupler design uses a miniature planar waveguide Rowland spectrometer configuration as the basic building block. The geometry of the Rowland device is

shown in Figure 1. The structure consists of a low-loss planar optical waveguide with a pair of cylindrical surfaces. The back surface, which supports a reflection grating, has a radius of curvature, R . The opposite surface comprises the Rowland Circle locus to which the input and output fibers are attached is located a distance, R , away from the grating and has a radius of curvature, $R/2$. The Rowland spectrometer combines the operation of a diffraction grating with a concave mirror to achieve spectral point-to-point imaging. By the incorporation of a planar waveguide, optical radiation is essentially confined to a two-dimensional plane which eases the fiber alignment problem while enhancing the durability of the structure. It should be noted that the Rowland Circle approximation is only valid for near axial rays in which the focal offset distance shown is minimal. In a compact two-dimensional Planar Wavelength Division Multiplexer with large aperture and incidence angles the Rowland Circle approximation tends to break down. Rays which originate and are diffracted by the circularly curved grating from large and/or unequal focal offset distances show significant path length differences and do not converge on the Rowland Circle locus.

During the first twelve months of the program, as reported in the first and second semiannual reports, we reviewed the basic design of the coupler-decoupler modules and completed the mechanical construction of the test set structure that houses the waveguide, the detectors and the lasers. We identified a central flaw layer in thin, hot-formed commercial glass sheets used as the guiding layers of the Rowland devices that may create severe aberration problems. Consequently, we developed a grinding and polishing process so that thicker glass sheets can be used and so that the flaw layer is polished away in the final guiding structure. We also completed the fabrication of precise master laps required to prepare the cylindrical ends of the Rowland module. In addition, a number of solutions were

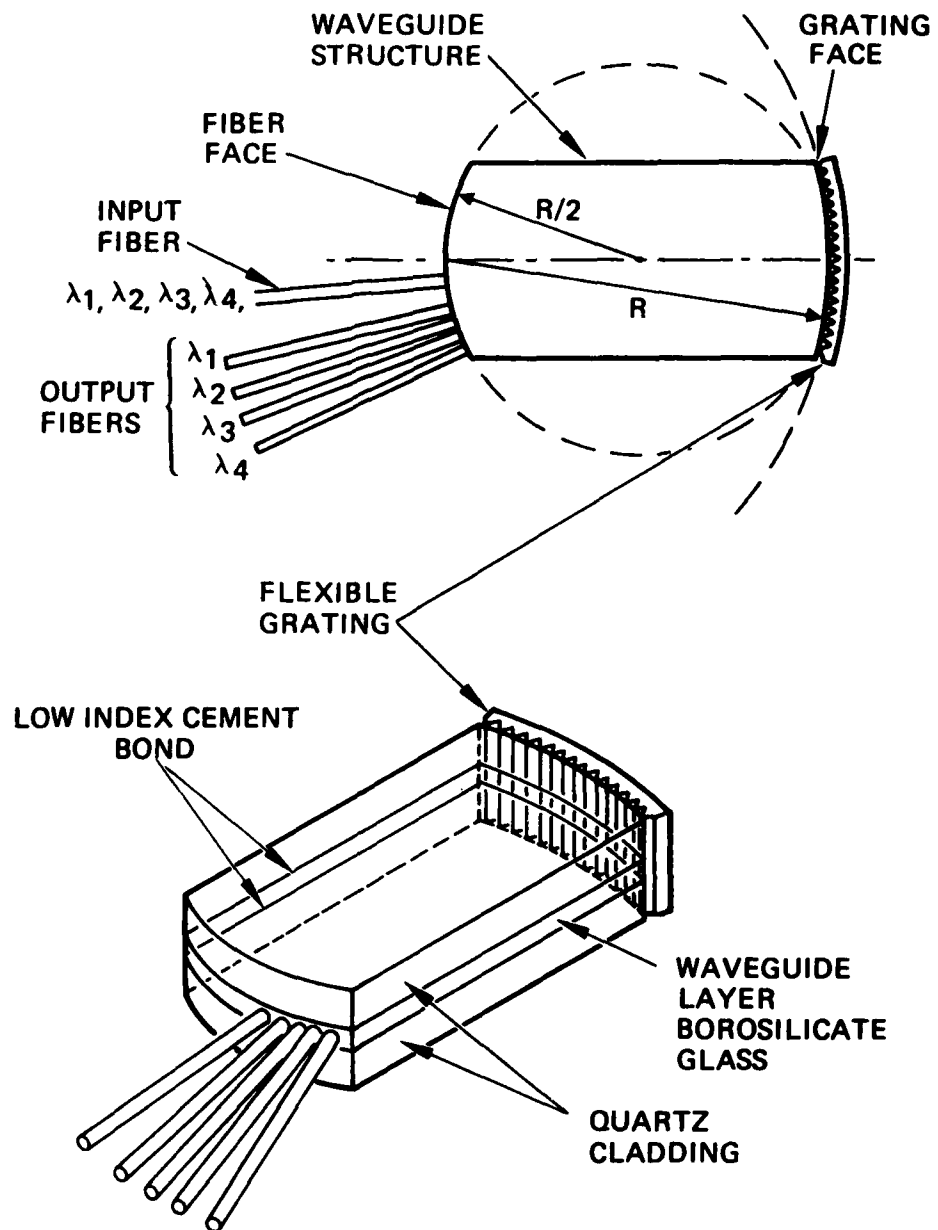


Figure 1. Planar waveguide Rowland coupler-decoupler.

developed for technical problems that were encountered during the waveguide fabrication process, including the cementing of glass layers.

We developed a laminating process (patent disclosure submitted) for forming a reliable bond of optical quality and low refractive index ($n_d = 1.463$). The excellent mechanical strength of this bond aggravated the effects of thermal coefficient of expansion mismatch between the core glass layer and the cladding glass layer of the planar waveguide. Component glasses of our previously selected pair had been chosen for optical properties alone, with no consideration for their thermomechanical properties. The core glass was selected for its low index in order to reduce Fresnel losses at the fiber-to-planar waveguide transition, and the cladding glass was selected for an index that would provide the best numerical aperture match. As a result, the thin borosilicate core glass layer, with its much larger thermal coefficient of expansion (than that of the thick quartz layer), was under great tensile stress during cooling after hot laminating. Excellent adhesion and the large coefficient mismatch combined to generate tensile forces which were large enough to rupture the thin core layer.

The requirement to match coefficients of thermal expansion was therefore added to the specifications of the two planar waveguide glasses. A pair of glasses with approximately the desired properties was selected and ordered. In this pair the thin core layer is under compression after cooling, which should eliminate the tensile rupture problem.

We made preliminary experiments on the holographic formation of blazed gratings on single crystal silicon wafers.

A new, simple and promising alternate approach to the formation of short focal length gratings was found with the help of our supplier of ruled gratings. We were able to obtain ruled, blazed precision replica gratings on flexible microscope cover glass substrates. Early experiments on these gratings

showed efficiencies in excess of 70% and good channel separation. Low cost is an attractive feature of these thin replica gratings.

During the third half-year period of the program the special glasses comprising near-index matched pairs were received. Sandwiches of the glass were laminated with TPX and the first lot was thinned in the optical shop. No fracture occurred in the thin guiding layer even though it was ground to a thickness of far less than is required for this application. However, it was found that the thinning process is extremely time consuming and costly, using up to 24 manhours of grinding and polishing for a single assembly.

Early bonding experiments in which unsupported replica gratings were bonded to a flexible plastic substrate gave disappointing results. These gratings stretched and wrinkled in an irregular manner and the attachment glue line contained bubbles. As a result, diffraction patterns of these gratings showed ghosts and sidelobes.

To eliminate this problem, we followed up on our early experiments of the previous reporting period and placed an order for replica gratings supported on thin microscope cover glasses. However, the microscope cover glass substrates on the first bath were too thick, and when these gratings were bent to the Rowland cylinder radius a large percentage fractured. Another order for gratings on thinner substrates was placed and was received toward the end of the present reporting period. Early measurements on this second lot of gratings showed lower efficiencies (as low as 50%). The manufacturer subsequently acknowledged the introduction of a new baking cycle to accelerate the replica separation process which may have been the cause of grating deterioration. A new lot of gratings was then manufactured without this high temperature baking cycle and should be performed with high efficiency. Our search for an extra thin flexible glass substrate for the gratings met with failure and

we therefore have returned to unsupported replica gratings made by the new low temperature process.

Reevaluation of our experimental results at the half-way mark showed that the attainment of a low loss planar waveguide with a bilateral numerical aperture match is far more difficult than anticipated. In order to conserve resources, further work on this promising component was curtailed and is being pursued in a parallel company-funded effort. A simpler planar waveguide design has been substituted in order to proceed within the time frame of the present contract. In this design planar waveguides are laminated with a thin, ready-made microscope cover glass guide layer, making their assembly much less labor-intensive. In this design only the grinding and polishing of the cylindrical Rowland surfaces involves special skills. Both in-house and commercial optical shops were evaluated for the preparation of these critical surfaces.

Toward the end of this reporting period we have made measurements of the diffraction efficiency of flexible gratings when the gratings were attached to the waveguide body by different methods. Diffraction plots on the chosen method at 632.8 and 825.5 nm showed good reproducibility with repeated applications. A novel process for precisely positioning the output fibers was implemented and proven.

During the next period we plan to acquire commercial modules for the laser transmitter and photodetector receiver and develop an improved tunable multiplexer input and output tap.

SECTION 2

EVALUATION OF REPLICA GRATINGS

As described in the previous interim report, we have chosen a replicated grating on a thin substrate as the diffraction element for the mini Rowland multiplexer. We are continuing the holographic grating studies in a longer term company-funded effort. A cooperative grating manufacturer has been very helpful in our search for an optimal grating structure. Initially, and as described in the previous report, we attempted to bond the bare replicated metal grating onto a flexible substrate after replication. This method turned out to be much too difficult. We then requested that the replicas be formed directly on a thin substrate. The change introduced the problem of substrate breakage. It appears that on the one hand, thin substrates, which are needed for easy cylindrical deformation, break during replica separation, while on the other hand, thick substrates which are needed for easy replica separation break during conforming cylindrical flexing. It therefore becomes necessary to develop a better replica forming process which permits easy separation of thin substrate replicas. The first such process was tried during the last reporting period and involved exposing the replicas to high temperature. This exposure degraded the diffraction efficiency of the replica grating. The measured diffraction efficiency into the desired -1 order was 50 to 60% down from the 70% efficiency obtained with earlier gratings. To date, several iterations of the replica grating formation have been carried out. A low temperature replicating process has now been introduced by the manufacturer and yields better results on substrate-less gratings.

Along with grating evaluation, we have also been developing the proper techniques for applying the grating to the curved waveguide endface. The key here is to ensure that the flexible

grating exactly follows the waveguide end curvature. Using a laminated waveguide together with a fixture that houses the waveguide, we have carried out experiments in an effort to understand the various factors that affect the diffracted beam spot size. The experimental arrangement is similar to that shown in Figure 2. One or two laser outputs were coupled into a 50 μm core multimode fiber which is butt-coupled to the input port of the demultiplexer. At the output of the demultiplexer, a 100- μm -core fiber was scanned across the face of the device and the optical power collected was recorded as a function of fiber position. Typical output scans are shown in Figure 3. The left trace shows the result of poor grating attachment and is characterized by a broad base and lower peak intensity. The right hand trace shows the output from a good grating attachment as a function of fiber position. We will continue with this effort until a method is developed for consistent and reproducible results.

In late 1983 we encouraged the HRL model shop management to invest in a rotating accessory for their electric discharge machine. This tool has now been received and has been used to drill the first 150 micrometer diameter holes on 200 micrometer centers in 1.6 mm thick aluminum. These holes appear perfectly round under a scanning electron microscope and show great promise as precisely located fiber positioners in the multiplexer. Experiments are now under way to reduce the taper of the holes and gain further experience with the process.

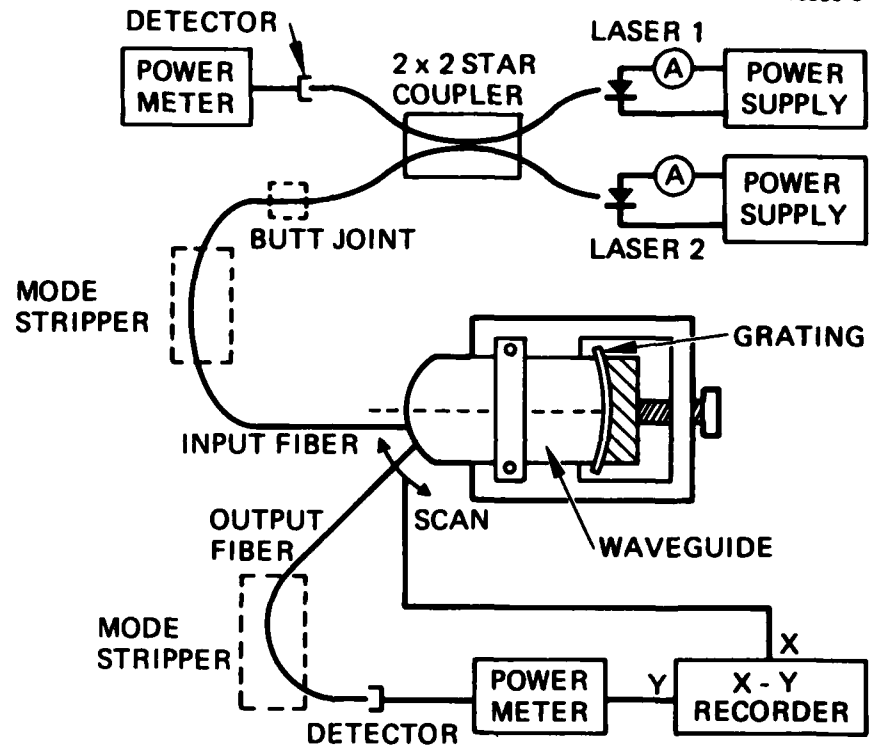


Figure 2. Experimental arrangement for grating attachment evaluation.

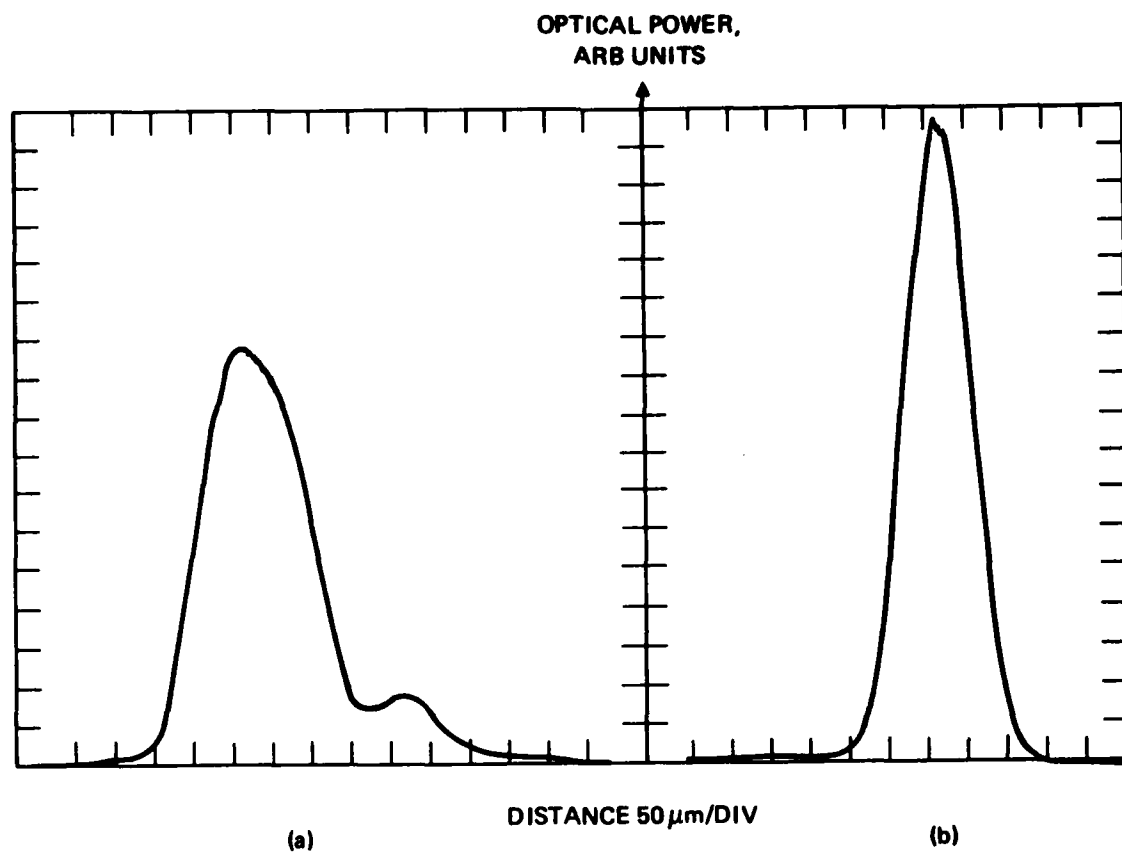


Figure 3. Output traces of a grating demultiplexer;
(a) with improper grating attachment;
(b) with proper grating attachment.

SECTION 3

PLANAR WAVEGUIDE FABRICATION

A. WAVEGUIDE LAMINATION

Early fabrication experiments on low loss planar waveguides with low loss and bilateral numerical aperture match showed the costliness of the required material and processes and forced a reorientation of the present program toward a more limited and economical approach. Efforts to obtain a core glass layer with a refractive index closely matching the fiber core index, and a bonding and cladding combination providing a matching numerical aperture, were therefore deferred to a parallel company-funded effort. Instead, readily available low cost Corning microscope cover glass are being used as the planar waveguide layer and precision soda lime plate glass, bonded with high temperature epoxy cement, is used to form the planar cladding. This simple waveguide assembly is economical to manufacture, but will, of course, be less efficient optically. Increased optical losses in this simple assembly are caused by a large index and numerical aperture mismatch at the input and output coupling sites, as well as by the absorption and scattering losses in the epoxy cladding layers and the central flaw layer in the core glass. (See first interim report).

During this reporting period we have completed all the lamination processes for planar waveguides. A thin microscope cover glass was sandwiched between two soda lime glass plates using optical epoxy cement. The glass plates have a dimension of 2 in. by 4 in. In order to laminate over this relatively large area with a minimum of air bubbles special precautions were taken. First, a thorough degreasing and cleaning of the component glass plates was carried out to remove any dirt or dust particles. Then the epoxy was prepared and degassed in a vacuum chamber. This particular step turned out to be the key in eliminating air bubbles in the finished structures. After

pouring the epoxy, the glass plates were folded together; the residual air bubbles trapped between the plates during this process were then squeezed out manually. The bonded structure was then further compressed (either a lead weight or a spring loaded plunger can be used). About 2 hours are required for the epoxy to cure completely before the finished structure can be removed from the press.

Since the cylindrical Rowland surface formation is best suited to batch processing, we have accumulated the laminated waveguides and waxed them into blocks ready for edge grinding and polishing.

B. CYLINDRICAL ROWLAND SURFACE FORMATION

The majority of optical surfaces formed in fabricating lenses and mirrors are spherical, thus most optical grinding and polishing tools are designed to form spherical surfaces. Early in the present program we foresaw the need for special optical tooling required to form cylindrical Rowland surfaces on the ends of the planar waveguide of the multiplexer. We designed and built precision self-correcting convex cylindrical master laps for subsequent use in the preparation of concave cylindrical lapping tools.

We selected radii of curvature of 75 mm and 37.5 mm, making the length of the Rowland waveguide 75 mm. These dimensions are a compromise between the contradictory requirements imposed by the need for ease of manufacture, minimum spot size, grating flexure, insensitivity to glass inhomogeneities, and minimum bulk.

Dimensions of the Rowland planar waveguide body are illustrated in Figure 4.

Two batches of the blocked waveguides were processed. One lot of 20 Rowland bodies was received from an outside vendor and one lot of 17 bodies was completed in the HRL optics shop. The optical quality of the cylindrical surfaces is comparable and

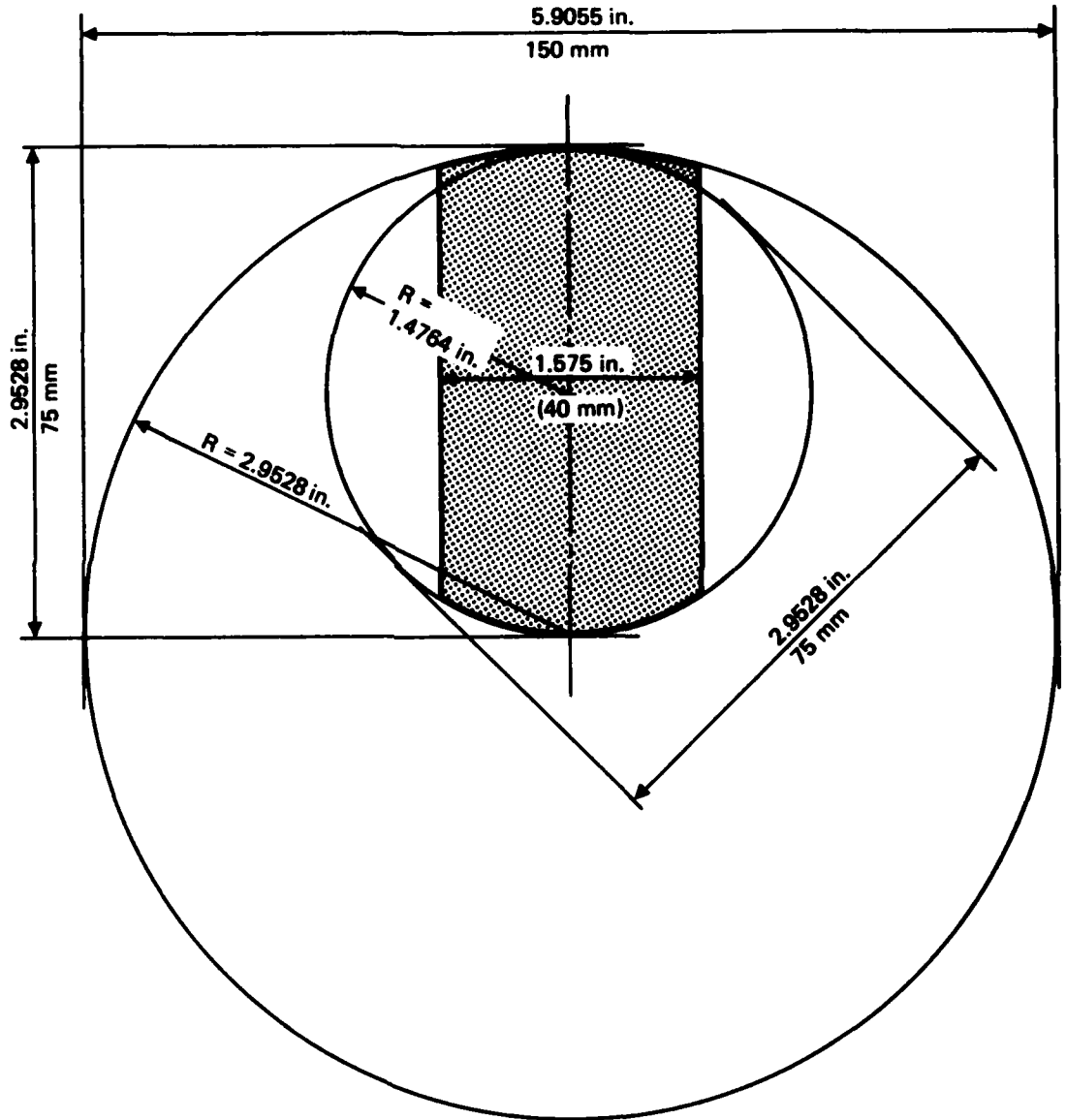


Figure 4. Dimensions of the Rowland planar waveguide under fabrication.

quite good in both lots. The outside vendor lot has slightly fewer edge chips but exhibit slight delamination around the edges. The HRL lot has slightly more chips but includes several units which did not delaminate. Unfortunately we are unable to make a valid optical comparison between the two lots because a new batch of a supposedly proven epoxy cement was introduced at an unknown point in the laminating bonding process. We subsequently found that this new batch was of inferior quality. We have no record of the bonding batch identity in the two lots and cannot make meaningful comparison measurements.

The finished waveguides will be characterized for their throughput efficiency according to the test plan. The best devices will be selected for the construction of deliverable coupler-decouplers.

SECTION 4

INTERNAL OPTICS OF THE MULTIPLEXER BODY

During our efforts to reduce the insertion loss of the wavelength division multiplexer and enhance the isolation of the separate signal channels we started an analysis of the internal optics of the Rowland body planar waveguide.

To determine the beam divergence angle and internal numerical aperture of the planar waveguide we made one way throughput measurements on a complete unit. The attached Figures 5 and 6 show the results of these angle measurements when a 50 micrometer core 0.26 N.A. fiber input is used. Measurements were made at both 6328 Å and 8255 Å wavelength and showed a cone angle of 18°. Since the refractive index of the core glass is 1.522 the internal numerical aperture of the planar waveguide is shown to be 0.238. At the grating distance of 75 mm the width of the illuminated grating area is:

$$\sim \tan 18^\circ \times 75 \text{ mm} = 25 \text{ mm}$$

indicating that the 40 mm wide grating is not completely filled, and that we can, if necessary use shorter gratings for the multiplexer.

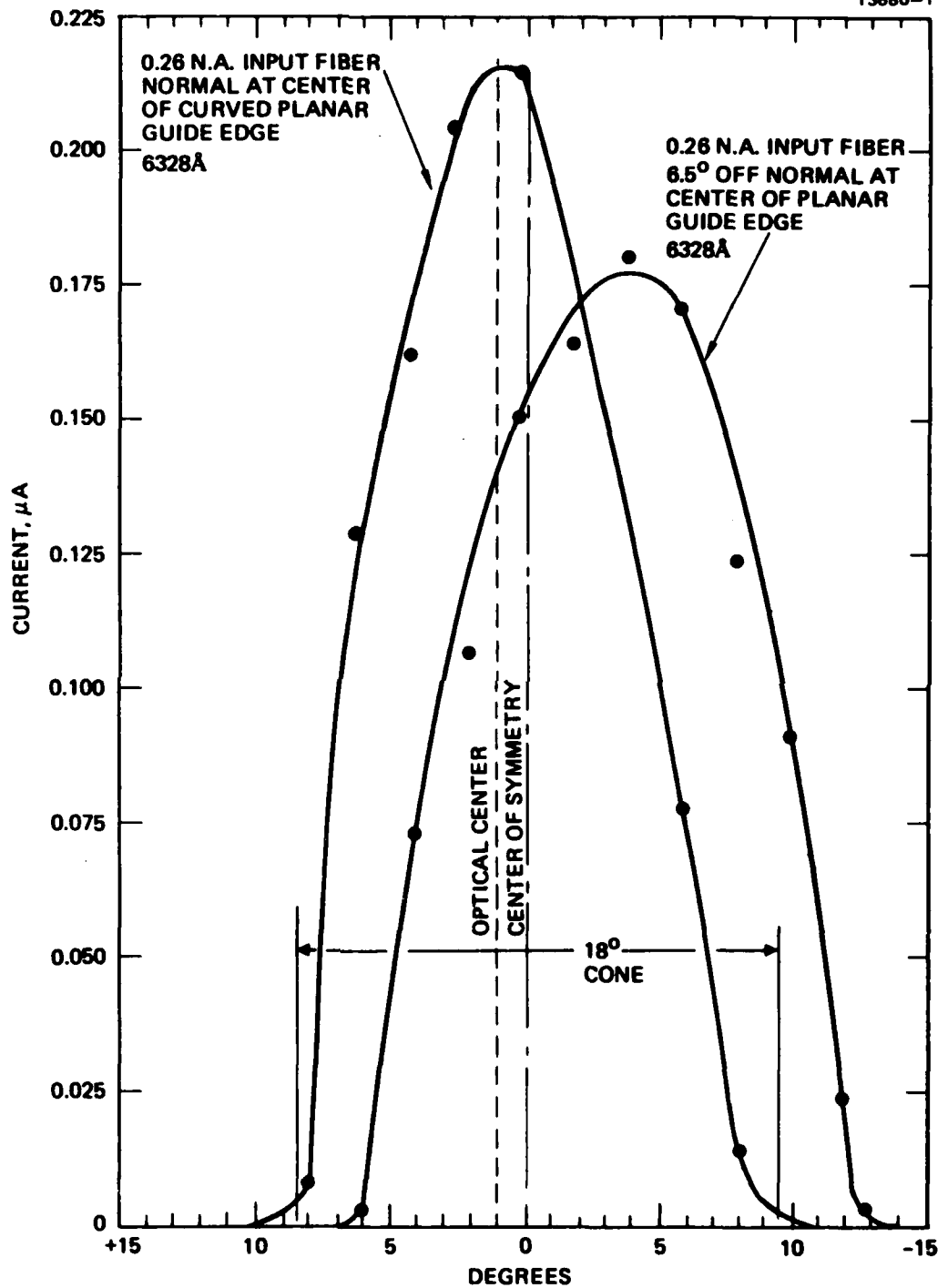


Figure 5. The light cone in the planar waveguide at 632.8 nm wavelength.

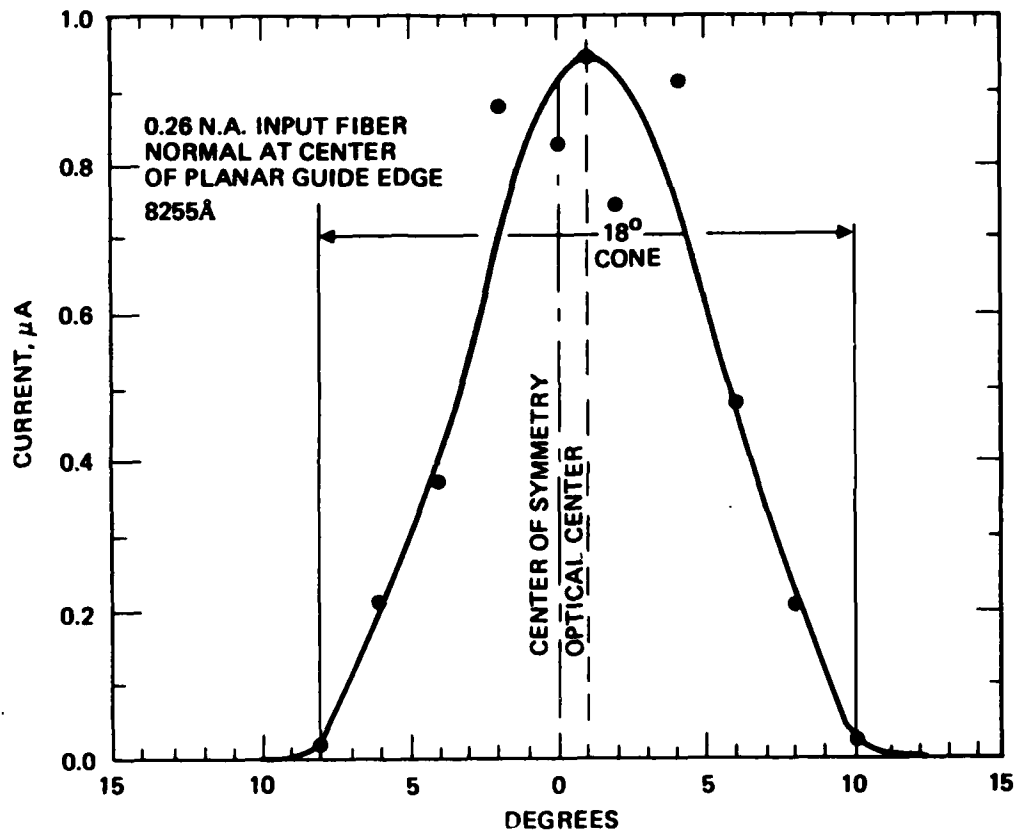


Figure 6. The light cone in the planar waveguide at 825.5 nm wavelength.

SECTION 5

THE ROWLAND CIRCLE GEOMETRY

The American physicist Henry Augustus Rowland (1841-1901) invented the concave diffraction grating used in spectroscopy. In his reflection grating spectrograph no auxiliary optics except a slit and a camera are needed. A circularly concave grating both collimates and focuses the light falling on it.

As shown in Figure 7, light which passes through a slit and falls on such a curved grating is dispersed by it into spectra which are supposed to be in focus on the Rowland Circle locus. On closer examination it becomes apparent that the Rowland Circle locus is an approximation which only holds for long focal lengths and small angle, near-axial rays.

This is caused by the fact that with larger offset distances the desired grating curvature must become elliptical, with the focal offset distance becoming the focal length of the ideal elliptically curved grating.

It is well known that light or sound emanating from the first focus of an elliptically curved surface will be reflected from that surface and reconcentrated at its second focus. The circularly curved grating surface of a Rowland spectrograph is only an approximate substitute for this ideal elliptical surface and this approximate substitution is only valid for near axial rays.

The absence of any auxiliary optical elements was the reason for selecting the Rowland geometry in the Multiwavelength Bidirectional Coupler-Decoupler design. By combining this geometry with a planar waveguide structure an attractive simple rugged configuration was obtained. However the small dimensions of the multiplexer and the relatively large working angles introduce very large path length errors and corresponding aberrations. Even an ideal elliptically curved grating can diffract only a single wavelength from a

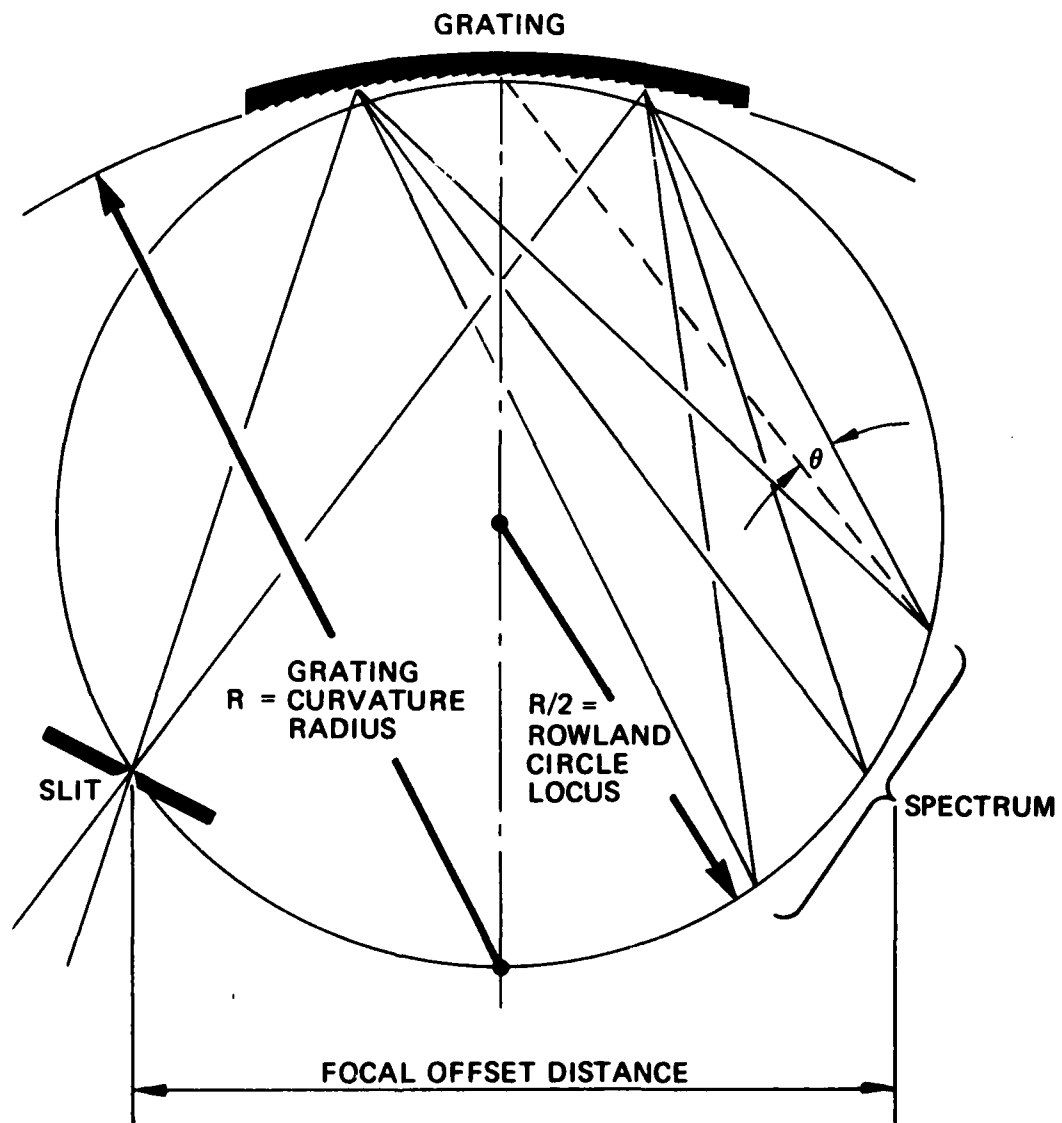


Figure 7. The Rowland Circle.

predetermined input port to a predetermined output port. Other wavelengths will diffract at different angles and cannot be focused by the grating ellipse. This is shown by analyzing the construction of the present Rowland Planar waveguide multiplexer body illustrated in Figure 8. A circular grating radius R representing an approximation of the ideal elliptical grating curvature forms the grating arc ADB centered at H . A smaller circle with the radius $R/2$ is centered at Z on the axis of the body halfway between the center, H , and the grating pole, D , and forms the Rowland Circle locus. We attempt to reduce path-length differences by diffracting the grating spectrum into the minus one order. In this manner we can keep the input and output ports close together and maintain small diffraction angles. However, the circular grating arc ADB which only approximates the ideal ellipse still introduces large aberrations because the major axis VW of the ideal ellipse, which passes through the input and output ports is severely tilted as shown. As a result, only a fraction of the grating area is in focus for both the input and output ports. Our study on this optical aberration continues in the hope of finding an alternate configuration of the multiplexer body. This search has not been successful yet.

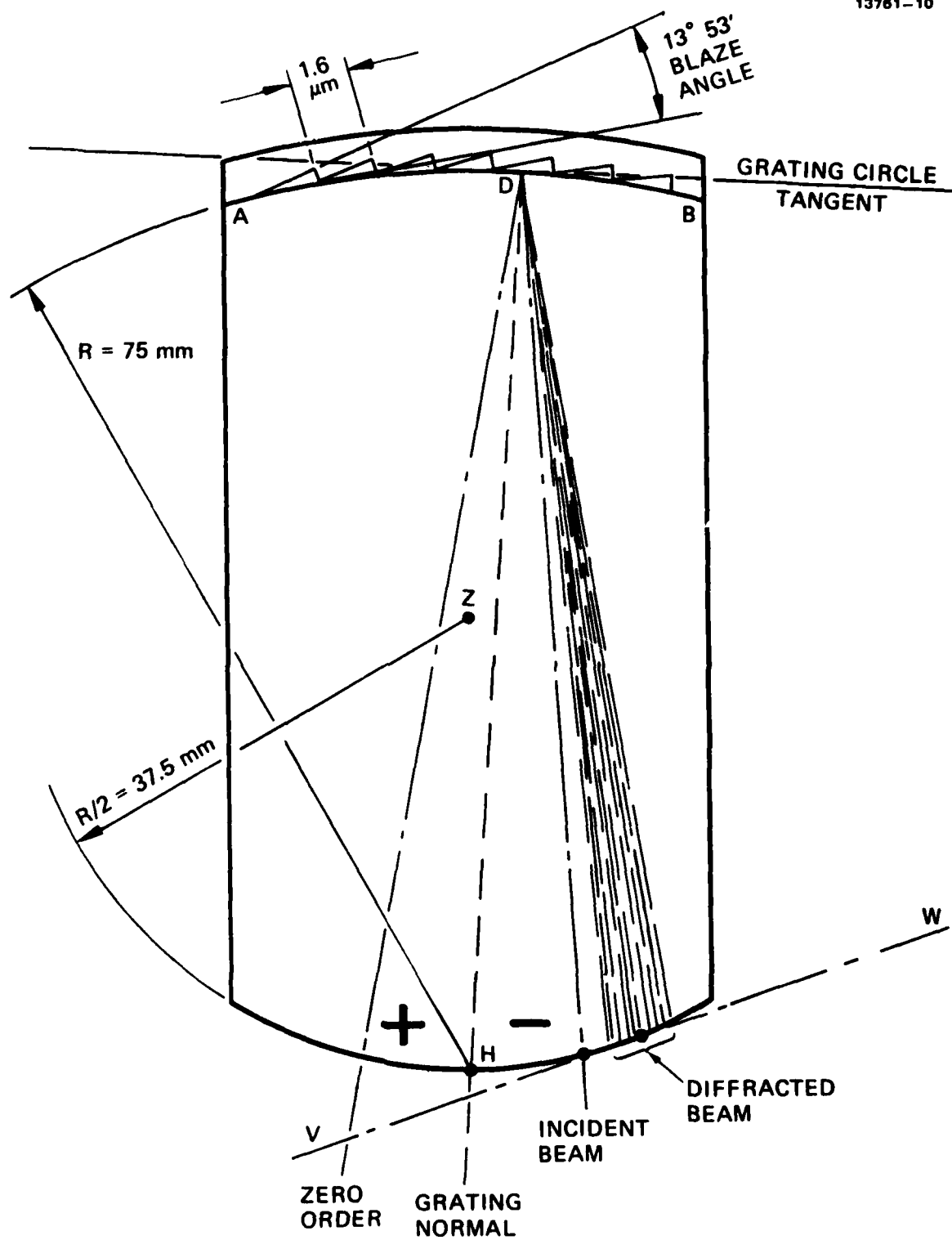


Figure 8. The present Rowland multiplexer geometry.

SECTION 6

COUPLER-DECOUPLER ASSEMBLY DESIGN

During this reporting period, we have carried out a number of experiments on measuring the diffraction efficiency of flexible gratings as described in Section 2. Simultaneously, we are also developing the techniques of mounting the gratings to the waveguide permanently.

The gratings were cut to appropriate size and mounted on the waveguide bodies with Scotch tape for initial testing. A 50 μm core fiber was used to illuminate the device with 8255 \AA radiation and the output spot was scanned using a 100 μm core fiber. Reasonably good traces were obtained for these gratings. It was also noticed that excessive pressure applied to the grating is not desirable, since it can cause additional structures in the output trace.

We developed a method of securing the waveguide body inside an aluminum fixture as shown in Figure 9.

We first tried to fill up the space with Eccofoam FDH, hoping that the pressure developed during the foaming process would be sufficient to press the grating firmly against the guide. However, it was found that the pressure developed was far too little.

After a few more attempts using different foaming agents we settled on a process that yielded fairly consistent results. One fine pitch pressure screw was installed in the waveguide fixture and used to apply pressure to the grating through a contour block and a plastic pressure pad (Sylgard 182). The fine pitch screw allows some tunability and minimizes the output spot size which is the criterion for optimization.

The completed waveguide-grating structure was characterized by exciting it with a 50 μm -core fiber carrying 0.83 μm radiation and plotting the output intensity from a 100 μm -core fiber as it was scanned across the output port of the device. We were able to

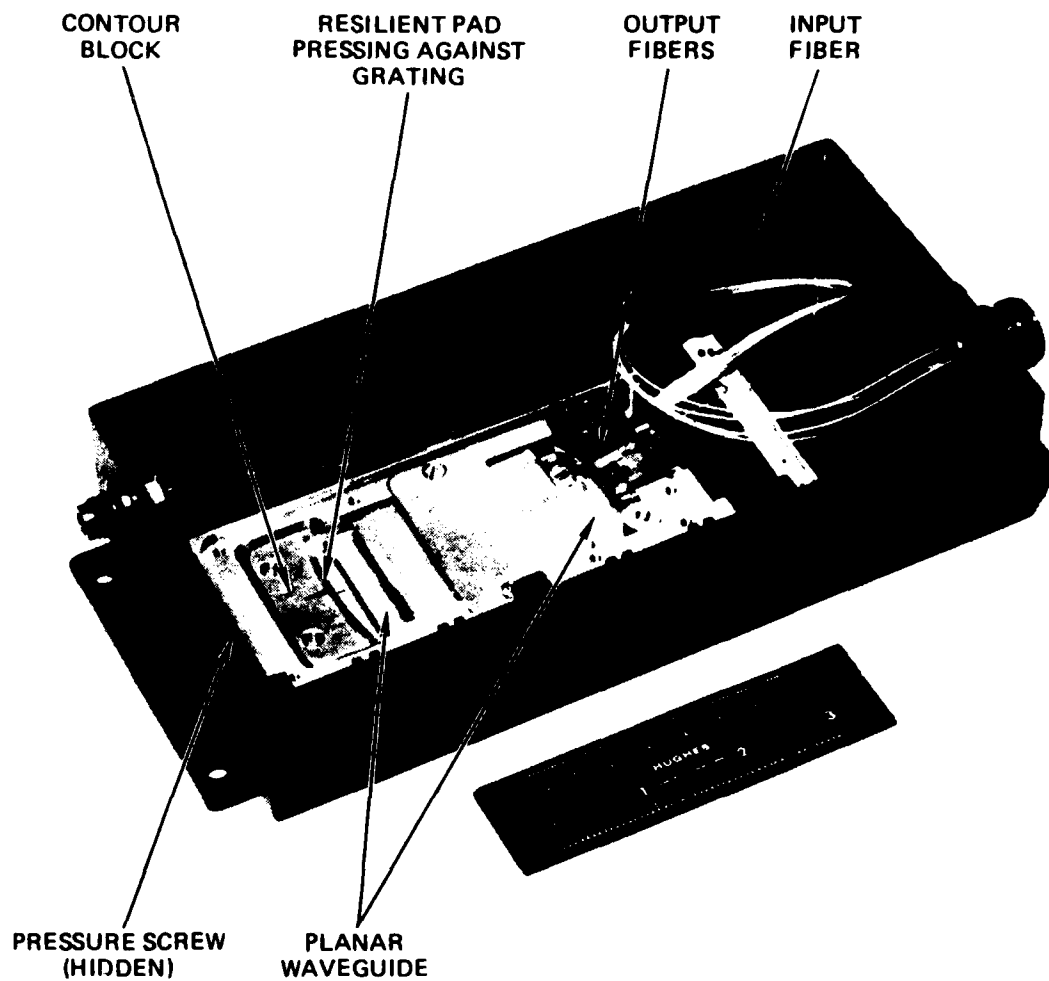


Figure 9. Typical demultiplexer assembly.

obtain similar traces from repeated applications of the grating to the waveguide indicating good reproducibility. A typical trace is shown in Figure 10.

Note that the traces are not symmetric. We believe that the long tail is due to intrinsic aberrations of the Rowland structure. We have also obtained some quantitative measures of the module insertion loss-ranging from 7.2 to 9 dB, as well as the crosstalk isolation - about 20.5 dB, for output fibers 300 μm apart. Both the insertion loss and crosstalk performance of the demultiplexers should improve when index matching epoxy is used between the fibers and the planar waveguide.

This particular approach of grating attachment appears to be quite stable and efficient. In the next few months we will continue to seek improvements of this baseline design.

During this reporting period we also started to study the method of positioning multiple input or output fibers for the decouplers. Since it is impractical to try to align each of the four fibers individually, we decided to use a linear fiber array at the output port. The array contains four output fibers at the desired spacing. In principle, one can use fiber spacers of different outer diameters to obtain any desired output fiber spacing. However, our initial results indicated that if the difference between the fiber diameters is too large, it becomes difficult to keep the small diameter fibers in their proper positions. Best results were obtained by using spacer fibers with the same diameter as the array fibers.

At HRL we have developed a unique method of encapsulating fiber arrays in copper through an electro-forming process. This process yields a rigid structure that can be mounted directly in the demultiplexer module.

Figure 11 shows the photo of the polished end of such a 4-fiber linear array. The fibers are completely surrounded by copper and are spaced exactly by one fiber diameter. We believe this is a viable approach to aligning multiple fibers to the

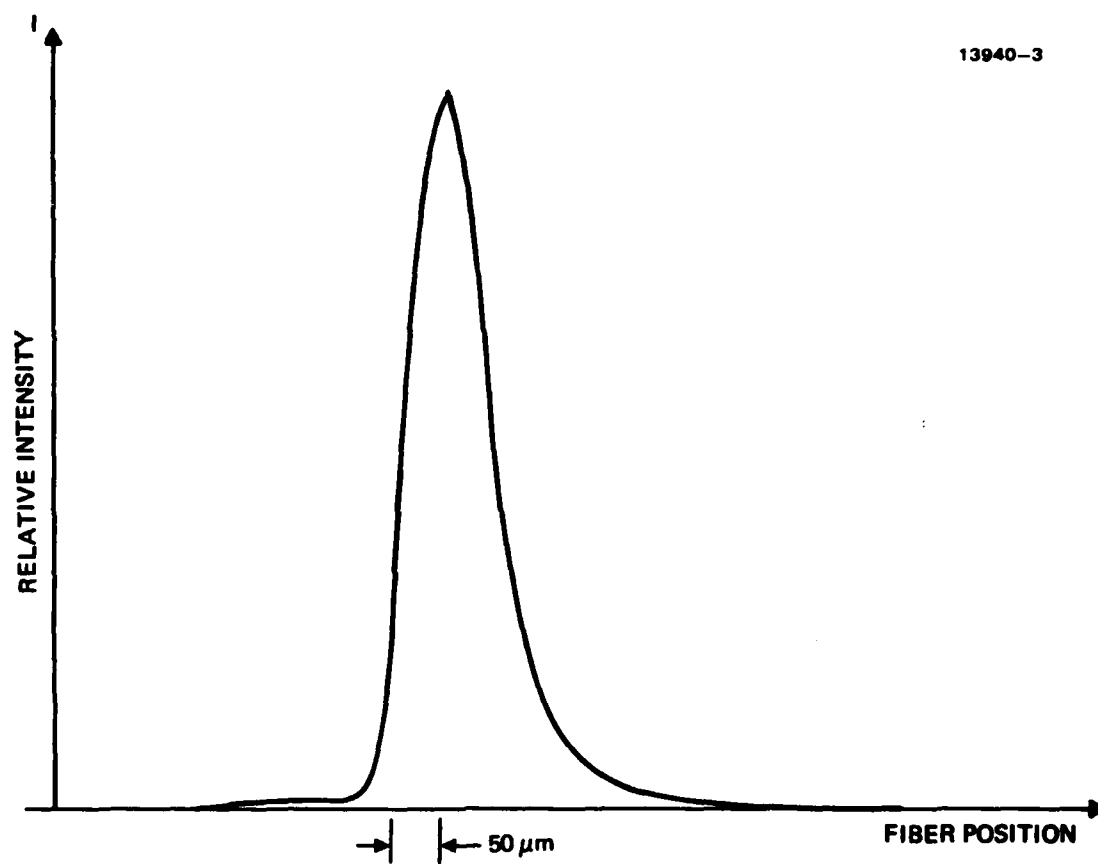


Figure 10. Collected optical power from the output fiber as a function of fiber position.

13940-2

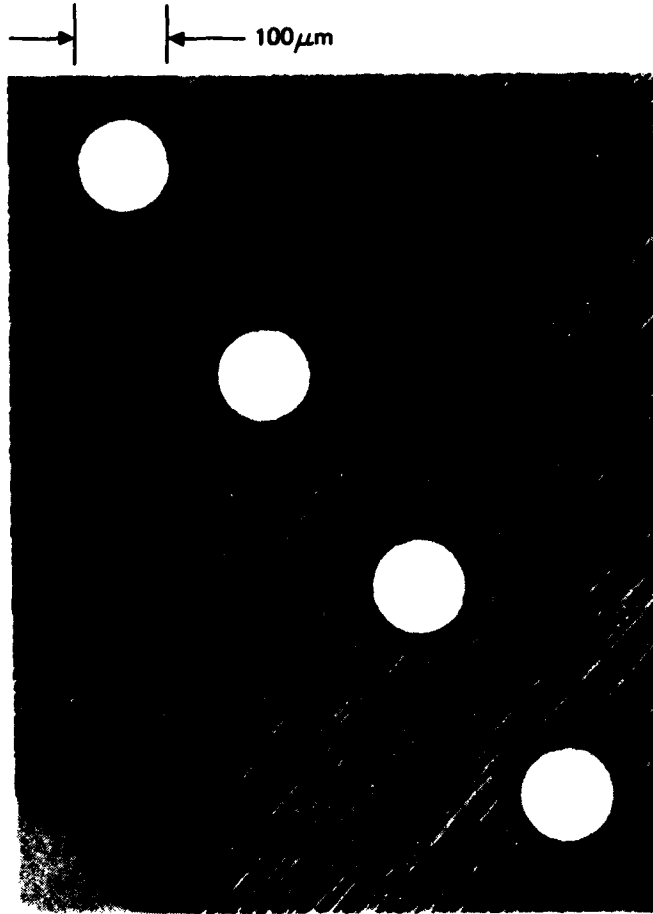


Figure 11. Polished end of fiber array.

coupler-decoupler modules. An alternative approach employing fiber holders using microscopic holes formed by electric discharge machining is also being investigated. The detailed arrangement for adjusting the location of the fiber array in relation to the waveguide is still under study and should be completed soon.

SECTION 7
FUTURE PLANS

We have completed the waveguide fabrication processes - lamination of the waveguide sandwiches and grinding and polishing of the cylindrical surfaces. The next step is to carefully characterize them optically and to select the best waveguides for final device assembly.

We have had substantial experience in handling the replica gratings on thin glass and epoxy substrates. In the meantime methods of attaching gratings to the waveguide with good optical contact while avoiding damage to the grating surface are also being developed. We will continue to perfect these procedures. We have started to work on the packaging designs for the coupler-decouplers. Particular emphasis are placed on fiber attachment and optical alignment procedures. Our initial design exhibited satisfactory results but there is still room for improvement.

We have decided to use commercial electronic modules for the laser transmitter and the photodetector receiver rather than design and build our own. A market survey showed that a 20 megabit (or megabaud) data rate, or the equivalent analog frequency response, represents the current state of the art of commercial devices. Higher frequency responses or data rates are being sought but are not yet available. Orders for these components will be placed during the next report period.

Design for the deliverable multiplexer network is now complete. Figure 12 shows the chosen configuration. Three such networks will be built as part of the present contract.

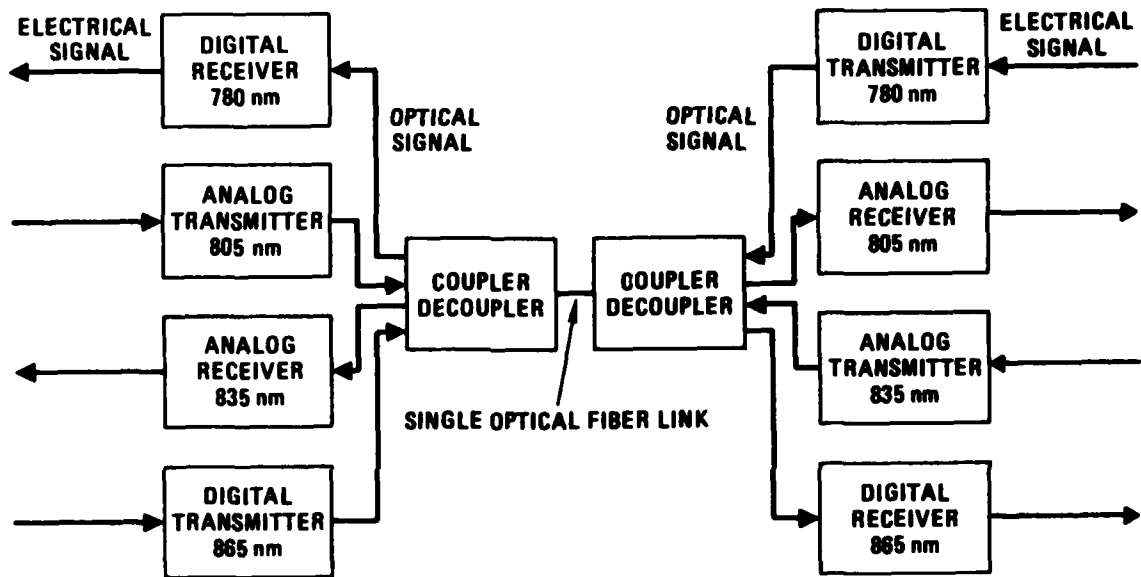


Figure 12. Multiplexer network.

This Page is Blank

DISTRIBUTION LIST

Defense Technical Info Center
Attn: DTIC-TCA
Cameron Station (Building 5)
Alexandria, VA 22314
(2 Copies)

Director, National Security
Agency ATTN: TDL
Fort George G. Meade, MD 20755

Code R123, Tech Library
DCA Defense Comm Eng. Ctr.
1860 Wichle Avenue
Reston, VA 22090

Defense Communications Agency
Technical Library Center
Code 205 (P.A. Tolovi)
Washington, DC 20305

Office of Naval Research
Code 427
Arlington, VA 22217

CIDEP Engineering & Support
Department, TE Section
P.O. Box 398
Norco, CA 91760

Director
Naval Research Laboratory
ATTN: Code 2627
Washington, DC 20375

Commander, Naval Electronics
Electronics Laboratory Center
ATTN: Library
San Diego, CA 92152

Command, Control &
Communications Division
Development Center
Marine Corps Development &
Education Command
Quantico, VA 22134

Naval Telecommunications
Command, Technical
Library, Code 91L
4401 Massachusetts Ave, NW
Washington, DC 20390

Rome Air Development Center
ATTN: Documents Library (TILD)
Griffiss AFB, NY 13441

AFG/SULL
S-29
Hanscom AFB, MA 01731

DCR, MIRCOCM
Readstone Scientific Info Center
Attn: Chief, Document Section
Redstone Arsenal, AL 35809

Commander
HQ Fort Huachuca
ATTN: Technical Reference Div.
Fort Huachuca, AZ 85613

Commander, US Army
Electronic Proving Ground
ATTN: STEEP-MT
Fort Huachuca, AZ 85613

Commander
USASA Test & Evaluation Center
ATTN: IAO-CDR-T
Fort Huachuca, AZ 85613

Director, US Army
Air Mobility R&D Lab.
Attn: T. Gossett, Bldg 207-5
NASA Ames Research Center
Moffett Field, CA 94035

HQDA (DAMO-TCE)
Washington, DC 20310

Deputy for Science & Technology
Office, Assist Sec Army (R&D)
Washington, DC 20310

HQDA (DAMA-ARP/DR. F.D. Verdame)
Washington, DC 20310

Director
US Army Human Engineering Labs
Aberdeen Proving Ground,
MD 21005

CDR, AVSCOM
ATTN: DRSVAV-E
P.O. Box 209
St. Louis, MO 63166

Director
Joint Comm Office (TRI-TAC)
ATTN: TT-AD (Tech Docu Cen)
Fort Monmouth, NJ 07703

Commander, US Army Satellite
Communications Agency
ATTN: DRCPM-SC-3
Fort Monmouth, NJ 07703

TRI-TAC Office
ATTN: TT-SE (Dr. Pritchard)
Fort Monmouth, NJ 07703

CDR, US Army Research Office
ATTN: DRXRO-IP
P.O. Box 12211
Research Triangle Park,
NC 27709

Commander, DARCOM
ATTN: DRCDE
5001 Eisenhower Avenue
Alexandria, VA 22333

CDR, US Army Signals
Warfare Laboratory
ATTN: DELSW-OS
Vinthill Farms Station
Warrenton, VA 22186

CDR, US Army Signals
Warfare Laboratory
ATTN: DELSW-AW
Vinthill Farms Station
Warrenton, VA 22186

Commander, US Army
Logistics Center
ATTN: ATCL-MC
Fort Lee, VA 22801

Commander, US Army
Training & Doctrine Command
ATTN: ATCD-TEC
Fort Monroe, VA 23651

Commander, US Army Training &
Doctrine Command
ATTN: ATCD-TM
Fort Monroe, VA 23651

NASA Scientific & Tech. Info.
Facility, Baltimore/Washington
Int'l Airport, P.O. Box 8757
Baltimore, MD 21240

Advisory Group on Elect. Devices
201 Varick Street, Ninth Floor
New York, NY 10014

Advisory Group on Elect. Devices
ATTN: Secy, Working Group D
(Lasers)
201 Varick Street
New York, NY 10014

TACTEC
Battelle Memorial Institute
505 King Avenue
Columbus, OH 43201

Ketron, Inc.
ATTN: Mr. Frederick Leuppert
1400 Wilson Blvd, Architect Bldg
Arlington, VA 22209

R.C. Hansen, Inc.
P.O. Box 215
Tarzana, CA 91356

CDR, US Army Avionic Lab
AVSCOM
ATTN: DVAA-D
Fort Monmouth, NJ 07703

Commander
RADC/DCLW
ATTN: T. Ross
Griffiss AFB, NY 13441

Commander, US Army Missile
R&D Command
ATTN: DRDMI-TDD (Mr. R. Powell)
Redstone Arsenal, AL 35809

Naval Ocean System Center
ATTN: Howard Rast, Jr., Code 8115
271 Catalina Blvd.
San Diego, CA 92152

Booz-Allen & Hamilton
ATTN: B.D. DeMarinis
776 Shrewsbury Avenue
Tinton Falls, NJ 07724

US Dept of Commerce
Office of Telecommunications
325 South Broadway
ATTN: Dr. R.L. Gallawa
Boulder, CO 80302

Naval Ocean Systems Center
Hawaii Laboratory
Box 997
ATTN: R. Seiple
Kailua, HA 96734

Defense Electronic Supply Ctr
ATTN: DESC-EMT (A. Hudson)
Dayton, OH 45444

The MITRE Corporation
P.O. Box 208
ATTN: B. Metcalf
Bedford, MA 01730

Project Manager, ATACS
ATTN: DRCPM-ATC
(Mr. J. Montgomery)
Fort Monmouth, NJ 07703

Commander
ERADCOM
ATTN: DELET-D
Fort Monmouth, NJ 07703

ATTN: DELSD-L-S (2 copies)

Commander, CECOM
ATTN: DRSEL-COM-D
Fort Monmouth, NJ 07703

ATTN: DRSEL-SEI

ATTN: DRSEL-COM-RM-1
(C. Loscoe) (21 copies)

Nasa Langley
ATTN: MS 477 (L. Spencer)
Hampton, VA 23665

GTE Communications System Div.
77 "A" Street
ATTN: J. Caggiano
Needham Heights, MA 02194

ITT Electro-Optical Prod. Div.
7635 Plantation Road
Roanoke, VA 24019

Bell Telephone Laboratories
Whippany Road
ATTN: Mr. G.A. Baker
Whippany, NJ 07981

Boeing Company
P.O. Box 3999-M/S 88-22
ATTN: O. MULkey
Seattle, WA 98124

Martin-Marietta Corporation
Denver Aerospace, P.O. Box 179
ATTN: G. Mangus
Denver, CO 80201

TRW Technology Research Center
2525 E. El Segundo Blvd.
ATTN: G. Mangus
El Segundo, CA 90245

Bell Northern Research
P.O. Box 3511, Station C
Ottawa, CANADA K1y 4H7

Frequency Control Products, Inc.
61-20 Woodside Avenue
ATTN: S. Reich
Woodside, NY 11377

END

FILMED

11-84

DTIC